Since January 2020 Elsevier has created a COVID-19 resource centre with free information in English and Mandarin on the novel coronavirus COVID-19. The COVID-19 resource centre is hosted on Elsevier Connect, the company's public news and information website.

International Journal of Biological Macromolecules 209 (2022) 984–990

Contents lists available at ScienceDirect

International Journal of Biological Macromolecules

journal homepage: www.elsevier.com/locate/ijbiomac

Expression, purification, and biophysical characterization of recombinant MERS-CoV main (M^{pro}) protease

Ghada Obeid Almutairi [a], Ajamaluddin Malik [a,*], Mona Alonazi [a], Javed Masood Khan [b], Abdullah S. Alhomida [a], Mohd Shahnawaz Khan [c], Amal M. Alenad [a], Nojood Altwaijry [c], Nouf Omar Alafaleq [a]

[a] Department of Biochemistry, College of Science, King Saud University, Riyadh, Saudi Arabia
[b] Department of Food Science and Nutrition, Faculty of Food and Agricultural Sciences, King Saud University, 2460, Riyadh 11451, Saudi Arabia
[c] Protein Research Chair, Department of Biochemistry, College of Science, King Saud University, Riyadh 11451, Saudi Arabia

ARTICLE INFO

Keywords:
MERS-CoV
Differential scanning fluorometry
Molten globule

ABSTRACT

MERS-CoV main protease (M^{pro}) is essential for the maturation of the coronavirus; therefore, considered a potential drug target. Detailed conformational information is essential to developing antiviral therapeutics. However, the conformation of MERS-CoV M^{pro} under different conditions is poorly characterized. In this study, MERS-CoV M^{pro} was recombinantly produced in *E.coli* and characterized its structural stability with respect to changes in pH and temperatures. The intrinsic and extrinsic fluorescence measurements revealed that MERS-CoV M^{pro} tertiary structure was exposed to the polar environment due to the unfolding of the tertiary structure. However, the secondary structure of MERS-CoV M^{pro} was gained at low pH because of charge-charge repulsion. Furthermore, differential scanning fluorometry studies of M^{pro} showed a single thermal transition at all pHs except at pH 2.0; no transitions were observed. The data from the spectroscopic studies suggest that the MERS-CoV M^{pro} forms a molten globule-like state at pH 2.0. Insilico studies showed that the covid-19 M^{pro} shows 96.08% and 50.65% similarity to that of SARS-CoV M^{pro} and MERS-CoV M^{pro}, respectively. This study provides a basic understanding of the thermodynamic and structural properties of MERS-CoV M^{pro}.

1. Introduction

Human coronaviruses were first characterized in the 1960s as the causative agents for generally mild to moderate respiratory infections. In 2003, the outbreak of novel human coronavirus causing severe acute respiratory syndrome (SARS) was reported as a global public health threat of the 21st century, severe-acute respiratory syndrome (SARS), and the virus was termed as SARS-CoV. SARS is an atypical form of pneumonia [1] that occurred in China and spread to 30 countries infecting more than 8000 people with a 10% case fatality rate (CFR) [2]. Another novel coronavirus causing severe acute respiratory syndrome emerged in the Middle East in 2012, with a higher CFR (35%), called Middle East respiratory syndrome (MERS-CoV) [2,3]. Recently in 2019 an outbreak of SARS-CoV-2 started in Wuhan City, Hubei Province of China, causing unusual viral pneumonia, recognized as coronavirus disease 2019 (COVID-19) [4]. SARS-CoV-2, which causes COVID-19 disease, quickly became pandemic due to direct human-to-human transmissions. As of November 08, 2021, COVID-19 infected over 248 million people and resulted in around 5 million deaths (https://covid19.who.int/).

Coronaviruses tend to mutate and infect several hosts. Therefore, they can jump between species and causes outbreaks in human and animals [5]. There are no effective antiviral drugs for human CoV infection [6]. Viral proteases are essential for the maturation of the viral proteins, thus vital for the coronavirus life-cycle [7]. MERS-CoV open-reading frame 1 (ORF1) encodes a papain-like cysteine protease (PL^{pro}) and main protease (M^{pro}, also called 3C-like cysteine protease, $3CL^{pro}$). Polyproteins pp1a and pp1b are cleaved by M^{pro}, which cleaves 11 sites, and PL^{pro}, which cleaves at three sites, to release sixteen mature nonstructural proteins involved in coronaviruses transcription and

Abbreviations: DTT, Dithiothreitol; IPTG, Isopropyl β-d-1-thiogalactopyranoside; Ni-NTA, Nickel-nitrilotriacetic acid; rpm, Rotation per minute.

* Corresponding author at: Department of Biochemistry, College of Science, Building no 5, room no 2A56, P.O. Box 2455, King Saud University, Riyadh 11451, Saudi Arabia.
E-mail address: amalik@ksu.edu.sa (A. Malik).

https://doi.org/10.1016/j.ijbiomac.2022.04.077
Received 24 February 2022; Received in revised form 4 April 2022; Accepted 11 April 2022
Available online 19 April 2022

replication [8,9]. Both M^{pro} and PL^{pro}, play an essential role in viral replication and maturation, making them attractive targets for discovering antiviral drugs [7,9].

MERS-CoV M^{pro} ($3CL^{pro}$) is a chymotrypsin-like cysteine protease, and because of its dominant role in the post-translational processing of the polyprotein, it is more commonly known as main protease (M^{pro}) [9]. MERS-CoV M^{pro} is a dimeric protein and has a conserved catalytic dyad (Cys148-His41) and an extended binding site consisting of a catalytic core (domain I and II) and a helical domain III [10]. In this study, recombinant MERS-CoV main protease (M^{pro}) was expressed and purified; various spectroscopic techniques were used for characterizing structural and thermodynamic properties of MERS-CoV M^{pro} at pH 1.0–7.0. The folded proteins are stabilized by different forces; therefore, characterizing protein stability is a significant challenge. Several methods (temperature, pH, chaotrops, ionic strength etc.) are used to characterize the protein stability [11]. In this study, we have tested the role of protonation in protein stability. In addition, insilico tools were used for comparative analysis of MERS-CoV M^{pro}, with its closest homologs (SARS-CoV M^{pro} and SARS-CoV-2 M^{pro}) at the sequence, structural and physicochemical level.

2. Methods

2.1. Chemicals and instruments

E. coli BL21(DE3)pLysS was used to express recombinant protein from Invitrogen; glycerol and NaCl came from Scharlau; Chicken egg white lysozyme was from Fluka; ANS, ampicillin, and benzonase were from Sigma and IPTG was purchased from Biobasic. NuPAGE 4–12% bis-tris-gel from Life technologies; pre-packed Ni-NTA column was from GE Healthcare Life Sciences. Cary 60 UV–Vis spectrometer and Cary Eclipse spectrofluorometer were from Agilent technologies, Innova 44R Shaking incubator was from New Brunswick, Thermomixer was from Eppendorf, and Circular dichroism spectroscopy (CD) was from Jasco.

2.2. Expression and purification of MERS-CoV M^{pro} in E.coli BL 21(DE3) pLysS

E.coli BL21(DE3)pLysS harboring codon-optimized pET 3a M^{pro} (Genscript) was used to express MERS-CoV M^{pro}. The expression and extraction of MERS-CoV M^{pro} from *E.coli* were performed as described in [10]. Briefly, recombinant MERS-CoV M^{pro} was purified using Ni-NTA pre-packed column (1 ml, GE Healthcare). Initially, cleared crude lysate was passed through the column pre-equilibrated with 20 mM Tris pH 8.0, 500 mM NaCl, 20% glycerol, and 30 mM imidazole and washed with 10 column volumes equilibration buffer. Next, bound protein was eluted with elution buffer (equilibration buffer containing 500 mM imidazole) at 1 ml min^{-1} flow rate. The protein-containing fractions were pooled and analyzed by SDS-PAGE. Pure fractions were collected and stored at -80 °C after adding 10% glycerol.

2.3. MERS-CoV M^{pro} quantification

Before analysis, purified MERS-CoV M^{pro} was thawed at room temperature and concentrated by using centricon tube at 4000 rpm for 40 min at 4 °C with three times buffer exchange (10 mM Tris pH 7.0, 50 mM NaCl). The absorbance of MERS-CoV M^{pro} was estimated at 280 nm, and the protein concentration was determined using an extinction coefficient of 43,890 M^{-1} cm^{-1}.

2.4. Exposure of MERS-CoV M^{pro} to different pHs

The protein was then diluted to 150 μg ml^{-1} with different buffers (pH 1.0 to 7.0) and equilibrated overnight at room temperature. The following buffers (30 mM each) were used; KCl-HCl (pH 1.0); Glycine-HCl (pH 2.0 and 3.0); Acetate (pH 4.0 and 5.0) and phosphate buffer (pH 6.0 and 7.0).

2.5. Fluorescence spectroscopy

Fluorescence spectra of MERS-CoV M^{pro} (1 μM) at different pH (1.0–7.0) were measured in a Cary Eclipse Fluorescence Spectrophotometer (Agilent Technologies) in a 1-cm path-length cuvette. The MERS-CoV M^{pro} samples were excited at 280 nm, and the fluorescence spectra were recorded in the range of 300–400 nm. Both excitation and emission slit widths were fixed at 10 nm. The changes in the surface hydrophobicity of MERS-CoV M^{pro} (1 μM) at different pHs were measured by adding 20 μM 8-Anilinonaphthalene-1-sulfonic acid (ANS). The samples were incubated at room temperature in the dark for 30 min before recording the fluorescence spectra. MERS-CoV M^{pro} samples at different pHs were excited at 385 nm (slit width set at 10 nm) and emission spectra were measured between 400 and 650 nm (slit width set at 10 nm). For aggregation studies of MERS-CoV M^{pro} at different pHs, Rayleigh scattering (RLS) measurement was performed at 25 °C by exciting samples at 350 nm (slit width 1.5 nm) and scanning the emission intensity between 300 and 400 nm with slit width at 2.5 nm.

2.6. Thermal shift assay

The thermal stability of MERS-CoV M^{pro} at different pHs was measured at 280 nm with 10 nm slit width, and the emission spectra were recorded between 310 and 360 nm (slit width 10 nm) in a Cary Eclipse Fluorescence Spectrophotometer. The temperature gradient used was 20–90 °C at a rate of 1 °C min^{-1}. The T_m values of MERS-CoV M^{pro} samples were obtained from the midpoint of the melting curve transition.

2.7. Circular dichroism (CD) measurements

Circular dichroism measurements were carried out by Jasco J-1500 CD spectropolarimeter. The temperature of the solutions was maintained at 25 °C. Far-UV CD spectra were recorded in the wavelength range (200–250 nm) using a quartz cuvette of 1 mm path-length filled with 0.4 ml of MERS-CoV M^{pro} (75 μg ml^{-1}) at different pH (1.0–7.0).

2.8. Insilico studies of M^{pro}

The amino acid sequences of different coronavirus (Covid-19 M^{pro}, GenBank: QRX35868.1; SARS M^{pro}, GenBank: AAR87511.1; MERS M^{pro}, GenBank: QLD98008.1) main-proteases were retrieved from the UniProt database [12]. Sequence similarity searches were performed using Position-Specific Iterated BLAST (PSI-BLAST) [13]. Closely related sequences of MERS-CoV M^{pro}, SARS-CoV M^{pro}, and SARS-CoV-2 M^{pro} were downloaded from the BLAST database. Multiple sequence alignment and visualization were performed using Jalview program version 2.11.1.3 [14]. The 3D structure and critical catalytic residues of MERS-CoV M^{pro} (PDB: 5C3N), SARS-CoV M^{pro} (PDB: 2BX4), and SARS-CoV-2 M^{pro} (PDB: 6Y2E) were analyzed using PyMOL. The physical and chemical characteristics (molecular weight, theoretical pI, amino acid composition, half-life, instability index, aliphatic index, and grand average of hydropathicity index (GRAVY)) of MERS-CoV M^{pro}, SARS-CoV M^{pro}, and SARS-CoV-2 M^{pro} were investigated using the ProtParam tool [15].

3. Results

3.1. Expression and purification of recombinant MERS-CoV M^{pro} in E. coli

MERS-CoV M^{pro} was overexpressed *in E. coli* BL21 (DE3) pLysS and purified via affinity chromatography as described in Bo-Lin et al. protocol [10]. In addition, the purity of eluted fractions was analyzed on SDS-PAGE. As shown in Fig. 1, MERS-CoV M^{pro} was expressed at a right

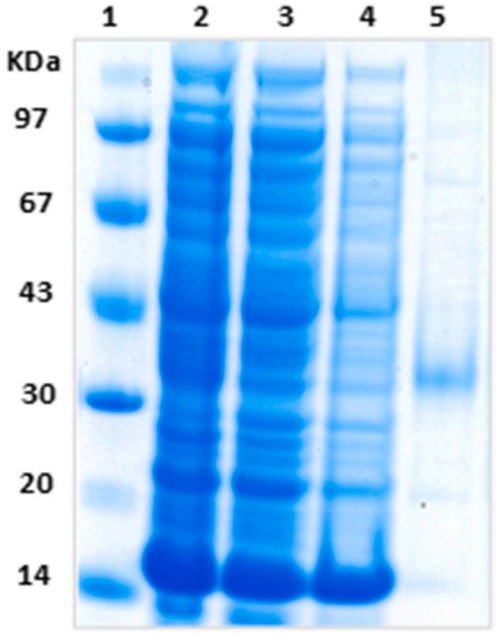

Fig. 1. Purification of His-tagged MERS-CoV M^{pro}. Lane 1, marker; lane 2, total cell lysate; lane 3, flow-through; lane 4, wash; lane 5, fraction 1.

size of 35.5 kDa.

3.2. Intrinsic fluorescence

Changes in the tertiary structure of MERS-CoV M^{pro} were monitored by analyzing changes in the intrinsic fluorescence emission. Intrinsic fluorescence usually occurs due to the fluorescent emission of tyrosine and tryptophan when excited at 280 nm [16]. Intrinsic fluorescence spectra of MERS-CoV M^{pro} at different pHs are shown in (Fig. 2A). The fluorescence spectra of the MERS-CoV M^{pro} at pH 7 showed maximum fluorescence intensity at 330 nm, which is the characteristic feature of folded proteins. However, MERS-CoV M^{pro} showed the highest fluorescent intensity (I_{max}) at pH 5.0 compared to at pH 7.0 at the same wavelength, i.e., 330 nm, indicating aromatic residues in the MERS-CoV M^{pro} moved towards a more hydrophobic environment. At pH 2.0, wavelength maxima (λ_{max}) was red-shifted almost 6 nm from 330 to 336 nm, indicating that the tertiary structure of MERS-CoV M^{pro} destabilized due to unfolding (Fig. 2B). Initially, the microenvironment around aromatic residues was relatively unchanged between pH 7.0 to 4.0. However, its conformation was destabilized below pH 4.0. Further protonation below pH 2.0 leads to gain of the native-like structure, as the λ_{max} was shifted back to native-like protein.

3.3. ANS binding assay

Extrinsic fluorescence was performed to identify the exposure of the hydrophobic patches on the MERS-CoV M^{pro} at different pHs. ANS is a hydrophobic sensitive dye that binds with proteins' hydrophobic regions. The ANS fluorescence intensity was found to increase when it was attached to the exposed hydrophobic patches. MERS-CoV M^{pro} at pH 7.0 showed lower ANS fluorescence but at pH 2.0 showed the highest fluorescent intensity (*I*max), suggesting that MERS-CoV M^{pro} at pH 2.0 is in a partially unfolded state (Fig. 3A). The ANS fluorescence intensity was plotted against different pHs (Fig. 3B). From Fig. 3B, it was seen that the ANS fluorescence intensity was slightly increased in the range of pH 7.0 to 4.0 (Fig. 3B). Below pH 4.0, ANS intensity was increased quickly, indicating a large increase in the surface hydrophobicity and maximum fluorescence intensity was found at pH 2.0. Later on, the ANS fluorescence intensity at pH 1.0 was returned to the fluorescence intensity of

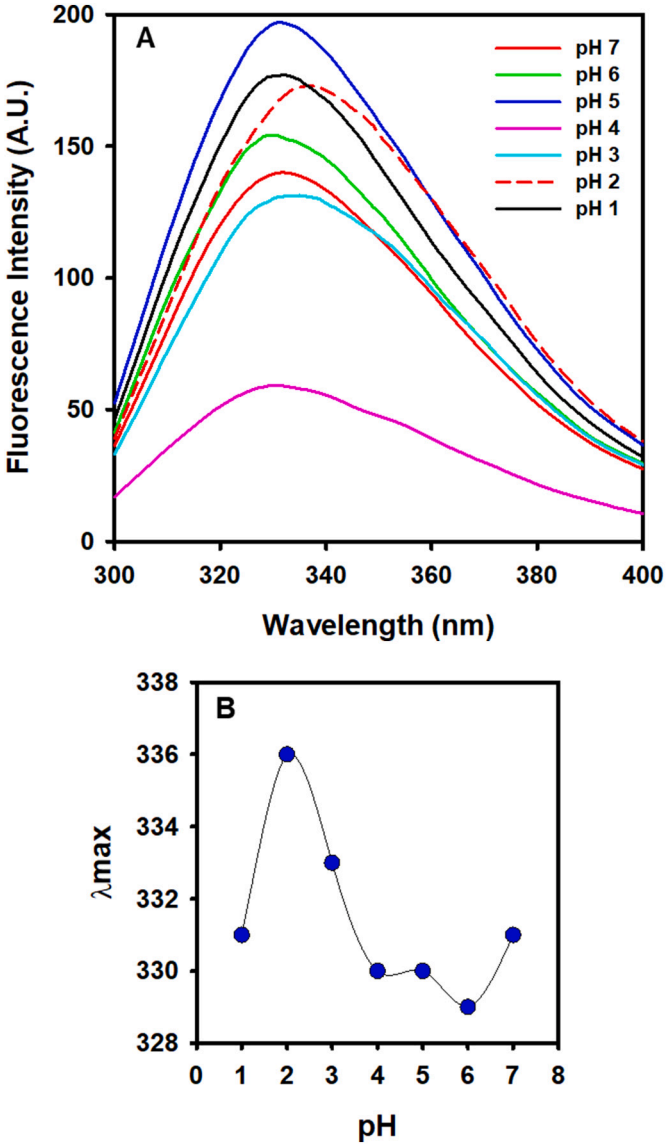

Fig. 2. Intrinsic fluorescence spectra of MERS-CoV M^{pro}. (A) Emission spectra of MERS-CoV M^{pro} at different pHs. An excitation wavelength of 280 nm was used and monitored emission in the range of 300–400 nm. (B) λ_{max} plotted with respect to pH.

native MERS-CoV M^{pro}, which designated that the MERS-CoV M^{pro} attained native-like folds.

3.4. Rayleigh light scattering (RLS) measurements

Rayleigh light scattering was performed to investigate pH-dependent MERS-CoV M^{pro} aggregation. Light scattering of samples was monitored at 350 nm after excitations of the same wavelength. As shown in Fig. 4, no significant increase in scattering intensity at 350 nm was observed across the entire pH range. Thus, MERS-CoV M^{pro} does not form aggregates at any pH.

3.5. Thermal shift assay

The thermal stability of MERS-CoV M^{pro} at pH 1.0–7.0 was monitored at 280 nm. The temperature was increased gradually from 20 to 90 °C at a constant rate of 1 °C min^{-1}, and the ratio of 350 nm/330 nm was plotted with respect to temperature (Fig. 5). MERS-CoV M^{pro} at all pHs shows a single transition, except at pH 2.0 no changes were

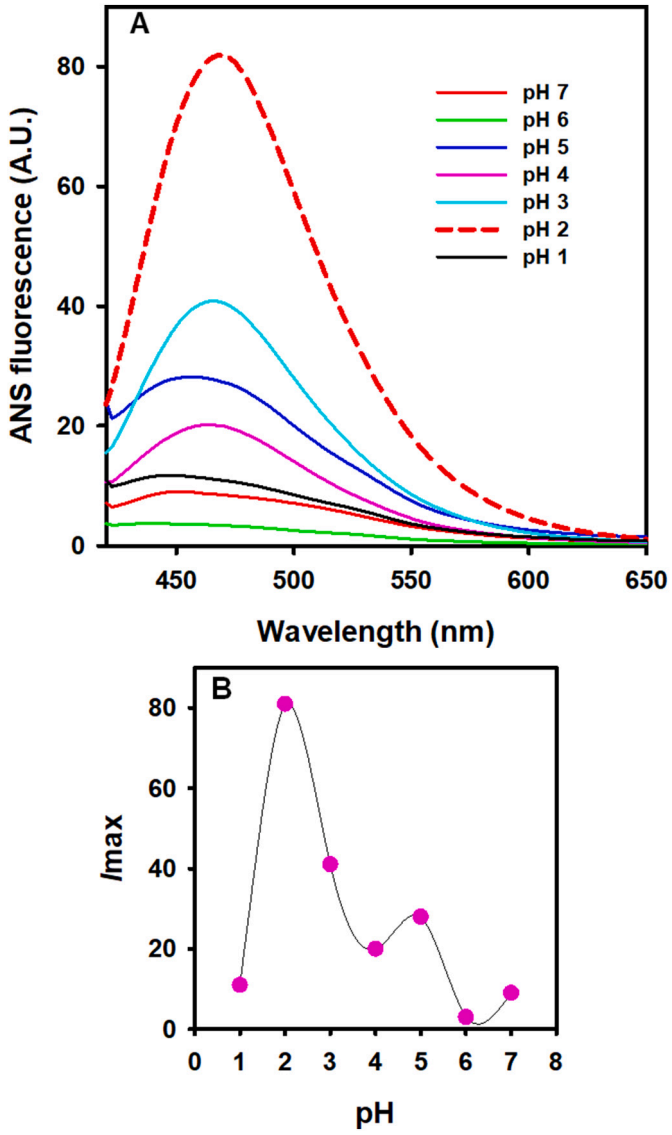

Fig. 3. Extrinsic fluorescence spectra of MERS-CoV M^{pro}. (A) Binding of ANS with MERS-CoV M^{pro} at different pHs. Samples were excited at 385 nm, and the spectra were recorded from 400 to 650 nm. (B) I_{max} plotted with respect to pH.

observed, and this result suggests that MERS-CoV M^{pro} at pH 2.0 lose tertiary structure and become partially unfolded. The thermal transition at pH 1.0 was very similar to the thermal transition of MERS-CoV M^{pro} at pH 7.0. The thermal shift assay also supports that the MERS-CoV M^{pro} at pH 2.0 is partially unfolded, and protein at pH 1.0 attained native-like stability. The thermal melting point (T_m) of MERS-CoV M^{pro} at different pHs is shown in Table 1.

3.6. Circular dichroism (CD)

Far UV-CD measurements studied changes in the secondary structure of MERS-CoV M^{pro}. The far-UV CD was measured in the range of 200–250 nm wavelength. The far-UV CD spectra of MERS-CoV M^{pro} at all pHs were plotted in Fig. 6. From Fig. 6, it was clear that the far-UV CD spectrum of MERS-CoV M^{pro} at pH 7.0 was characterized by two negative peaks at 208 and 222 nm, which is a characteristic feature of the α-helix. The secondary structure was nearly intact up to pH 5.0. Below it, there was a gain of another minimum at 218 nm, which indicated a formation of beta-sheet-like structure in the MERS-CoV M^{pro} at pH 2.0 and 3.0. Interestingly at pH 1.0, MERS-CoV M^{pro} regained native-like

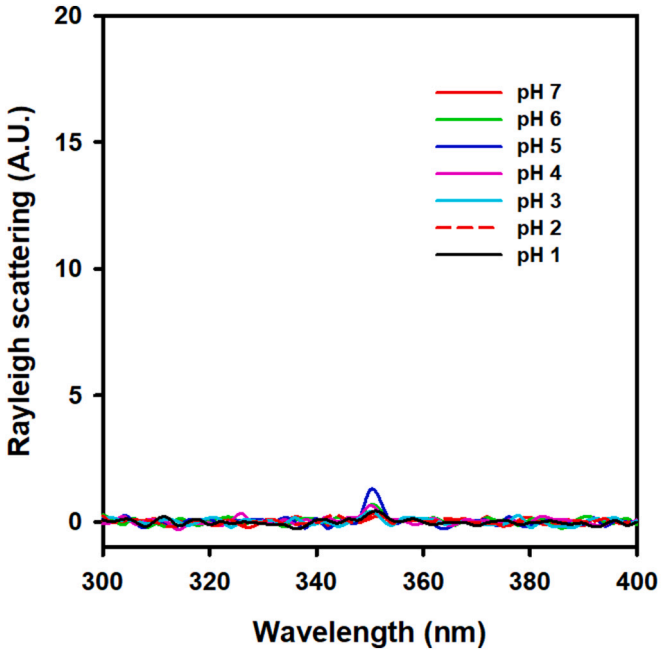

Fig. 4. Analysis of aggregate formation in MERS-CoV M^{pro} at pH 1.0–7.0.by RLS. MERS-CoV M^{pro} excited at 350 nm and emission spectra recorded between 300 and 400 nm.

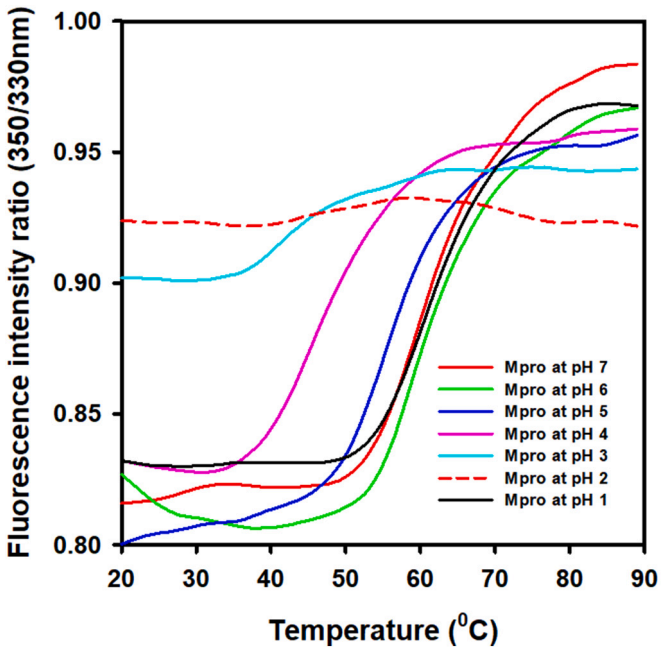

Fig. 5. The thermal shift assay for MERS-CoV M^{pro} at pH 1.0–7.0. MERS-CoV M^{pro} samples were continuously heated from 20 to 90 °C at 1 °C min^{-1} and the spectra were collected at the range of 310–360 nm. The ratio of 350 nm/330 nm was plotted as a function of temperature.

secondary structure.

3.7. Insilico studies of coronaviruses main protease

According to BLAST, MERS-CoV M^{pro} was conserved, with 100% identity among all MERS-CoV variants with the query cover of 100%, and 0 *E*-value (Supplementary fig. S1). Similar results were observed among all SARS-CoV M^{pro} variants (Supplementary fig. S2) and SARS-

Table 1
Thermal melting point (T_m) of MERS-CoV M^{pro} at pH 1.0, 4.0, 5.0, 6.0 and 7.0.

pH	T_m (°C)
1.0	61.9
2.0	N·D.
3.0	44.0
4.0	47.0
5.0	54.2
6.0	60.5
7.0	62.0

N.D: not determined.

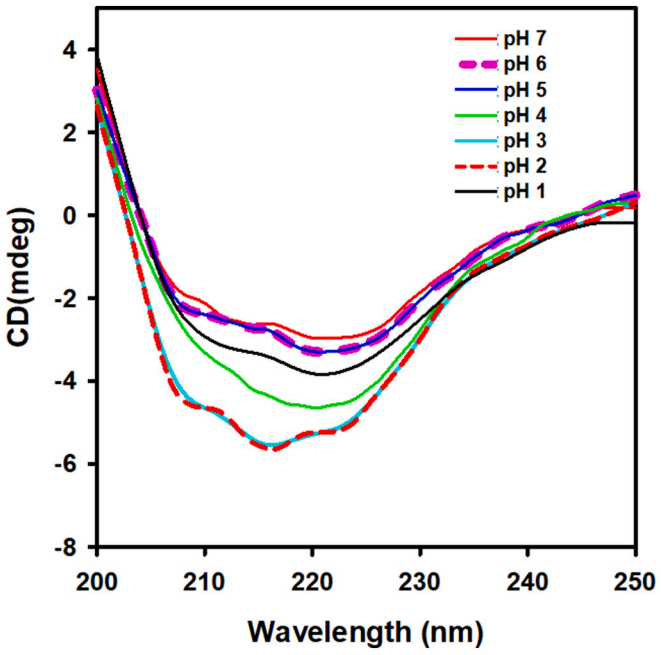

Fig. 6. Far UV CD studies of MERS-CoV M^{pro}. Far-UV CD spectra (200-250 nm) of 75 μg ml^{-1} MERS-CoV M^{pro} at pH 1.0 to 7.0.

CoV-2 M^{pro} variants (Supplementary fig. S3), indicating that the main protease was fully developed conserved within coronavirus sub-classes. Next, the MERS-CoV M^{pro} protein sequence was compared with its closest homologs (SARS-CoV and Covid-19). The results revealed that the number of amino acid residues was identical beginning from Ser1 to Gln306. SARS-CoV-2 M^{pro} shares identity percentages of 96.08% with Covid-19 M^{pro}, and the differences were at twelve positions in the sequence alignment. The sequence identity between Covid-19 M^{pro} and MERS-CoV M^{pro} was 50.65% (Table 2, Supplementary fig. S4). These results showed that the Covid-19 M^{pro} shared a higher sequence homology towards SARS-CoV M^{pro} than MERS-CoV M^{pro}. Finally, three different structural comparisons were performed (Supplementary fig. S5). The pairwise structural imposition of MERS-CoV M^{pro} with SARS-CoV M^{pro} (Supplementary fig. S5A) and with Covid-19 M^{pro} (Supplementary fig. S5B) indicates a lower degree of structural similarity and conservation of the catalytic dyads (Cys 148 instead of Cys 145) (Supplementary fig. S6), while SARS-CoV M^{pro} and Covid-19 M^{pro} exhibit nearly identical structures (Supplementary fig. S5C) with similar

Table 2
Protein BLAST result using SARS-CoV-2 M^{pro} as a query sequence.

Subject sequence	Query coverage	*E*-value	Identity
SARS-CoV M^{pro}	100%	0.0	96.08%
MERS-CoV M^{pro}	100%	5e-115	50.65%

catalytic dyad residues Cys145 and His41 (Supplementary fig. S6). ProtParam tool was used to compute parameters to analyze physicochemical properties of MERS-CoV M^{pro}, SARS-CoV M^{pro}, and Covid-19 M^{pro}. The results were shown in Table 3. Analysis of physicochemical properties revealed that the three main proteases, polypeptides are 306 amino acids long with a molecular weight of around 33.0 KDa. According to the theoretical pI, all M^{pro}s were negatively charged. The estimated half-life was more than 10 h for all M^{pro}. The instability index value for all M^{pro}s was found as stable. The aliphatic index showed that SARS-CoV-2 M^{pro} more thermally stable than MERS-CoV M^{pro} and SARS-CoV M^{pro} and a GRAVY was found negative in both Covid-19 M^{pro} and SARS-CoV M^{pro}.

4. Discussion

Preparing a purified and stable protein sample is a necessary procedure and is required before placing significant efforts into structural and biophysical studies. His-tagged recombinant MERS-CoV M^{pro} was successfully expressed in *E.coli* and purified by using affinity chromatography in this study. Biomass was prepared by following an optimized protocol [10]. His-tagged MERS-CoV M^{pro} was purified using Ni-NTA resin and detected by SDS-PAGE, and the position of the band was consistent with the calculated molecular weight of MERS-CoV M^{pro} (Fig. 1). This indicated that the target protein was expressed, and the His-tag expression system was suitable for purifying MERS-CoV M^{pro}.

Biophysical methods have been widely used to understand the structural properties, folding and protein stability [17,18]. This study employed a combination of techniques, including intrinsic and extrinsic fluorescence, Rayleigh scattering measurements, thermal shift assay, and far-UV CD. With these spectroscopic measurements, a pH range was applied to induce structural changes in the MERS-CoV M^{pro}. Intrinsic tryptophan fluorescence provides information about the local microenvironment of the tryptophan residue, which response very sensitively to any change of the protein tertiary structure [19]. The maximum fluorescent intensity of MERS-CoV M^{pro} at acidic pH 5.0 was observed at 330 nm (Fig. 2), suggesting that the tryptophan residues moved towards a more hydrophobic environment. At pH 2.0 the maximum fluorescence wavelength at 336 nm was observed, suggesting that the tertiary structure of MERS-CoV M^{pro} was partially unfolded at this pH. The wavelength maximum of MERS-CoV M^{pro} was red-shifted when pH lowered from neutral pH to pH 2.0. The red-shift of the maximum fluorescence peak resulted from changes in the tryptophan residues microenvironment from a non-polar to the solvent-exposed environment during the unfolding of the protein [20].

An extrinsic fluorescence dye (ANS) was used in this study. This extrinsic dye in an aqueous solution shows low fluorescence signals, but the fluorescence signals increase when exposed to a hydrophobic environment due to partially unfolded or aggregated proteins [21]. ANS emission spectra of MERS-CoV M^{pro} (Fig. 3) displayed the highest fluorescent intensity at pH 2.0, confirming that MERS-CoV M^{pro} at pH 2.0 is partially unfolded. It has been reported that ANS dye has a higher affinity to the partially unfolded state or molten globule (MG) state of the protein than that of the native and denatured states. Research has demonstrated the acidic pH-induced MG state in many proteins such as apo-α-lactalbumin, lipopolysaccharide-binding protein, and retinol-binding protein [22–24]. Further protonation below pH 2.0 leads to the gain of the native-like structure. The changes in intrinsic fluorescence (internal microenvironment) and extrinsic ANS fluorescence (Surface hydrophobicity) of MERS-CoV M^{pro} at different pHs were similar.

RLS intensity of a protein solution can be measured using a spectrofluorometer to detect the protein aggregation [30]. Our results showed that MERS-CoV M^{pro} remained soluble at the entire pH range (Fig. 4). The thermal stability of MERS-CoV M^{pro} was studied by thermal shift assay. MERS-CoV M^{pro} at all pHs exhibited a single thermal transition (Fig. 5). Exceptionally at pH 2.0, no transitions were observed,

Table 3
Physicochemical parameter results computed by ExPASy ProtParam.

Protein name	Number of amino acids	Molecular weight KDa	Theoretical PI	Total number of negatively charged residues (Asp+Glu)	Total number of positively charged residues (Arg + Ly)	half-life (hour) (*E. coli*)	Instability index (II)	Aliphatic index	GRAVY[a]
MERS-CoV M^{pro}	306	33.3	5.86	21	16	>10	27.33	79.90	0.129
SARS-CoV M^{pro}	306	33.8	6.22	26	23	>10	29.67	81.83	−0.049
SARS-CoV-2 M^{pro}	306	33.7	5.95	26	22	>10	27.65	82.12	−0.019

[a] GRAVY means the Grand average of hydropathicity.

and this result supports our finding that this protein obtained a partially unfolded state at pH 2.0. In a recent study, Covid-19 M^{pro} also undergoes a single thermal transition with similar folding behavior of MERS-CoV M^{pro} [25].

THE far-UV CD spectroscopy method is routinely used to rapidly determine the secondary structure of proteins and monitor dynamic changes of protein structure due to the straightforward sample preparation and fast acquisition time of this method [26]. In this study, the far-UV CD spectrum of MERS-CoV M^{pro} at pH 7.0 (Fig. 6) displayed two negative peaks at ~208 nm and ~ 222 nm, indicating alpha-helix dominant structure; the secondary structure was nearly intact up to pH 5.0. Below it, gain another minimum at 218 nm, which indicated a gain of beta-sheet-like structure in the MERS-CoV M^{pro} at pH 2.0 and 3.0. Similar results were observed in previous studies of SARS-CoV and SARS-CoV-2 main proteases when calculated secondary structure contents [25].

In this study, we have also evaluated the similarity between the three main proteases of MERS-CoV, SARS-CoV, and Covid-19 by using insilico tools to compare proteins based on sequence, structure, and physical, and chemical properties. This screening would be beneficial to drug screening researchers. Sequence alignment reported in (Supplementary fig. S1,2 and 3), shows a striking degree of conservation at an amino acid level among all M^{pro} variants. By aligning the multiple amino acid sequences of MERS-CoV M^{pro}, SARS-CoV M^{pro}, and Covid-19 (Supplementary fig. S4), we observed that these enzymes showed low conservancy MERS-CoV M^{pro} show only 50.65% sequence similarity with Covid-19 M^{pro}. In contrast, Covid-19 M^{pro} shows a higher sequence identity with the previous SARS-CoV M^{pro}, which is consistent with previous research results.

The 3D structures of MERS-CoV M^{pro}, SARS-CoV M^{pro}, and Covid-19 displayed the three main proteases containing a catalytic dyad consisting of a His residue and a Cys residue. MERS-CoV M^{pro} pairwise structural imposition to SARS-CoV M^{pro} (Supplementary fig. S5A) and to Covid-19 (Supplementary fig. S5B) indicates a comparatively lower degree of structural similarity and conservation of the catalytic dyads. The difference was in the Cys148 [10]. The structural imposition of Covid-19 M^{pro} and SARS-CoV M^{pro}, showed a difference in twelve amino acids and the obtained results showed that Covid-19 M^{pro} has a catalytic dyad (Cys145 and His41) consistent with SARS-CoV M^{pro} (Cys-145 and His-41), which exists precisely at a similar location [27]. A recent study demonstrated that the superimposition of SARS-CoV and Covid-19 main proteases exhibit a high degree of active site conservation [9].

Analysis of physicochemical parameters was computed for MERS-CoV M^{pro}, SARS-CoV M^{pro}, and Covid-19 (Table 3). Length and size (molecular weight) are the most fundamental characteristic of protein sequences. No variation in protein length and molecular weight were observed in our study among the three M^{pro}s. The isoelectric point and charge are also important parameters for solubility and interaction. It was observed that the theoretical pI was >7 for all M^{pro}, which indicates that all proteases are negatively charged and that it can be precipitated in acidic medium. Regarding the instability index value, all M^{pro} is classified as stable (instability index >40). Another measure for the stability of proteins is the aliphatic index. The aliphatic index is known as the volume of the protein occupied by the aliphatic side chain, and an increase in the aliphatic index value is reported to enhance the protein thermostability [28].

The aliphatic index of SARS-CoV-2 M^{pro} was 82.12, when compared to other M^{pro} inferred that SARS-CoV-2 M^{pro} was more stable under a wide range of temperature conditions.

It is also essential to determine the hydrophobic or hydrophilic character of the protein. In the case of SARS-CoV-2 M^{pro} and SARS-CoV M^{pro}, GRAVY scores were negative values indicating a low hydrophobic nature and good solubility. On the other hand, the MERS-CoV M^{pro} GRAVY score was a positive value showing greater hydrophobicity in nature, and the protein is sparingly soluble in water. This comparative analysis at the sequence, structural and physicochemical properties level could prove valuable for producing broad-spectrum main protease inhibitors. Protease inhibitors would be worth following as they may provide specific drugs for upcoming coronavirus outbreaks.

5. Conclusion

In conclusion, MERS-CoV M^{pro} at pH 2.0 exhibited a partially unfolded state. In addition, the thermal shift assay revealed that MERS-CoV M^{pro} unfolds via a single thermal transition at pH 7.0, and no transition was observed at pH 2.0. Moreover, Far-UV CD showed that MERS-CoV M^{pro} displayed a mixture of an α-helix and β-sheet structure at pH 7.0, and the secondary structure was modified at pH 2.0. Interestingly MERS-CoV M^{pro} regained all its secondary structure at pH 1.0. Similar CD spectrum and thermal stability results were also observed in Covid-19 M^{pro}. Finally, the *insilico* screening showed that M^{pro} is highly conserved between SARS-CoV and SARS-CoV-2, much more so than MERS-CoV M^{pro}.

CRediT authorship contribution statement

Ghada Obeid Almutairi: Data curation, Writing.
Ajamaluddin Malik: Conceptualization, Supervision, Writing, review & editing.
Mona Alonazi: Supervision, review & editing.
Javed Masood Khan: Methodology, Formal analysis, review & editing.
Abdullah S. Alhomida: Resources,
Mohd Shahnawaz Khan: Resources, review & editing.
Amal M. Alenad: Resources, review & editing.
Nojood Altwaijry: Funding acquisition, review & editing.
Nouf Omar Alafaleq: Resources, review & editing.

Acknowledgments

The authors thank the Deanship of Scientific Research, KSU, and the Chair for Protein Research for their continuous support.

Appendix A. Supplementary data

Supplementary data to this article can be found online at https://doi.

org/10.1016/j.ijbiomac.2022.04.077.

References

[1] J. Cui, F. Li, Z.L. Shi, Origin and evolution of pathogenic coronaviruses, Nat. Rev. Microbiol. 17 (3) (2019) 181–192.

[2] J.A. Al-Tawfiq, A. Zumla, Z.A. Memish, Travel implications of emerging coronaviruses: SARS and MERS-CoV, Travel Med. Infect. Dis. 12 (5) (2014) 422–428.

[3] J.A. Al-Tawfiq, A.S. Omrani, Z.A. Memish, Middle East respiratory syndrome coronavirus: current situation and travel-associated concerns, Front. Med. 10 (2) (2016) 111–119.

[4] P. Zhou, X.L. Yang, X.G. Wang, B. Hu, L. Zhang, W. Zhang, H.R. Si, Y. Zhu, B. Li, C. L. Huang, H.D. Chen, J. Chen, Y. Luo, H. Guo, R.D. Jiang, M.Q. Liu, Y. Chen, X. R. Shen, X. Wang, X.S. Zheng, K. Zhao, Q.J. Chen, F. Deng, L.L. Liu, B. Yan, F. X. Zhan, Y.Y. Wang, G.F. Xiao, Z.L. Shi, A pneumonia outbreak associated with a new coronavirus of probable bat origin, Nature 579 (7798) (2020) 270–273.

[5] P. V'Kovski, A. Kratzel, S. Steiner, H. Stalder, V. Thiel, Coronavirus biology and replication: implications for SARS-CoV-2, Nat. Rev. Microbiol. 19 (3) (2021) 155–170.

[6] A. Artese, V. Svicher, G. Costa, R. Salpini, V.C. Di Maio, M. Alkhatib, F. A. Ambrosio, M.M. Santoro, Y.G. Assaraf, S. Alcaro, F. Ceccherini-Silberstein, Current status of antivirals and druggable targets of SARS CoV-2 and other human pathogenic coronaviruses, Drug Resist. Updat. 53 (2020), 100721.

[7] R. Hilgenfeld, From SARS to MERS: crystallographic studies on coronaviral proteases enable antiviral drug design, FEBS J. 281 (18) (2014) 4085–4096.

[8] A. Kilianski, A.M. Mielech, X. Deng, S.C. Baker, Assessing activity and inhibition of Middle East respiratory syndrome coronavirus papain-like and 3C-like proteases using luciferase-based biosensors, J. Virol. 87 (21) (2013) 11955–11962.

[9] S. Ullrich, C. Nitsche, The SARS-CoV-2 main protease as drug target, Bioorg. Med. Chem. Lett. 30 (17) (2020), 127377.

[10] B.L. Ho, S.C. Cheng, L. Shi, T.Y. Wang, K.I. Ho, C.Y. Chou, Critical assessment of the important residues involved in the dimerization and catalysis of MERS coronavirus main protease, PLoS One 10 (12) (2015), e0144865.

[11] A. Malik, J.M. Khan, S.F. Alamery, D. Fouad, N.E. Labrou, M.S. Daoud, M. O. Abdelkader, F.S. Ataya, Monomeric Camelus dromedarius GSTM1 at low pH is structurally more thermostable than its native dimeric form, PLoS One 13 (10) (2018), e0205274.

[12] C. UniProt, UniProt: the universal protein knowledgebase in 2021, Nucleic Acids Res. 49 (D1) (2021) D480–D489.

[13] S.F. Altschul, W. Gish, W. Miller, E.W. Myers, D.J. Lipman, Basic local alignment search tool, J. Mol. Biol. 215 (3) (1990) 403–410.

[14] A.M. Waterhouse, J.B. Procter, D.M. Martin, M. Clamp, G.J. Barton, Jalview Version 2–a multiple sequence alignment editor and analysis workbench, Bioinformatics 25 (9) (2009) 1189–1191.

[15] M.R. Wilkins, E. Gasteiger, A. Bairoch, J.C. Sanchez, K.L. Williams, R.D. Appel, D. F. Hochstrasser, Protein identification and analysis tools in the ExPASy server, Methods Mol. Biol. 112 (1999) 531–552.

[16] J.M. Khan, A. Malik, P. Sen, A. Ahmed, M. Ahmed, S.F. Alamery, H.A. Almaharfi, H. Choudhry, M.I. Khan, Different conformational states of hen egg white lysozyme formed by exposure to the surfactant of sodium dodecyl benzenesulfonate, Int. J. Biol. Macromol. 128 (2019) 54–60.

[17] A. Malik, D. Fouad, N.E. Labrou, A.M. Al-Senaidy, M.A. Ismael, H.M. Saeed, F. S. Ataya, Structural and thermodynamic properties of kappa class glutathione transferase from Camelus dromedarius, Int. J. Biol. Macromol. 88 (2016) 313–319.

[18] J.M. Khan, A. Malik, A. Ahmed, M.T. Rehman, M.F. AlAjmi, R.H. Khan, S. Fatima, S.F. Alamery, E.M. Abdullah, Effect of cetyltrimethylammonium bromide (CTAB) on the conformation of a hen egg white lysozyme: a spectroscopic and molecular docking study, Spectrochim. Acta A Mol. Biomol. Spectrosc. 219 (2019) 313–318.

[19] A. Malik, A. Haroon, H. Jagirdar, A.M. Alsenaidy, M. Elrobh, W. Khan, M. S. Alanazi, M.D. Bazzi, Spectroscopic and thermodynamic properties of recombinant heat shock protein A6 from Camelus dromedarius, Eur. Biophys. J. 44 (1–2) (2015) 17–26.

[20] J.T. Vivian, P.R. Callis, Mechanisms of tryptophan fluorescence shifts in proteins, Biophys. J. 80 (5) (2001) 2093–2109.

[21] N.A. Al-Shabib, J.M. Khan, A. Malik, P. Sen, M.A. Alsenaidy, F.M. Husain, A. M. Alsenaidy, R.H. Khan, H. Choudhry, M.A. Zamzami, M.I. Khan, S.A. Shahzad, A quercetin-based flavanoid (rutin) reverses amyloid fibrillation in beta-lactoglobulin at pH2.0 and 358K, Spectrochim. Acta A Mol. Biomol. Spectrosc. 214 (2019) 40–48.

[22] K. Kuwajima, The molten globule state of alpha-lactalbumin, FASEB J. 10 (1) (1996) 102–109.

[23] P. Sen, B. Ahmad, R.H. Khan, Formation of a molten globule like state in bovine serum albumin at alkaline pH, Eur. Biophys. J. 37 (8) (2008) 1303–1308.

[24] E. Paci, L.H. Greene, R.M. Jones, L.J. Smith, Characterization of the molten globule state of retinol-binding protein using a molecular dynamics simulation approach, FEBS J. 272 (18) (2005) 4826–4838.

[25] O. Abian, D. Ortega-Alarcon, A. Jimenez-Alesanco, L. Ceballos-Laita, S. Vega, H. T. Reyburn, B. Rizzuti, A. Velazquez-Campoy, Structural stability of SARS-CoV-2 3CLpro and identification of quercetin as an inhibitor by experimental screening, Int. J. Biol. Macromol. 164 (2020) 1693–1703.

[26] A. Malik, S. Albogami, A.M. Alsenaidy, A.M. Aldbass, M.A. Alsenaidy, S.T. Khan, Spectral and thermal properties of novel eye lens zeta-crystallin, Int. J. Biol. Macromol. 102 (2017) 1052–1058.

[27] D.W. Kneller, G. Phillips, H.M. O'Neill, R. Jedrzejczak, L. Stols, P. Langan, A. Joachimiak, L. Coates, A. Kovalevsky, Structural plasticity of SARS-CoV-2 3CL M (pro) active site cavity revealed by room temperature X-ray crystallography, Nat. Commun. 11 (1) (2020) 3202.

[28] A. Ikai, Thermostability and aliphatic index of globular proteins, J. Biochem. 88 (6) (1980) 1895–1898.